

Pore pressure generation in sand with bentonite: from small strains to liquefaction

C. S. EL MOHTAR*, A. BOBET†, V. P. DRNEVICH‡, C. T. JOHNSTON‡ and M. C. SANTAGATA†

The paper examines the effect of small percentages of bentonite on pore pressure generation in loose sands, from small strains all the way to liquefaction. It relies on resonant column, static triaxial and cyclic triaxial tests conducted on specimens prepared by dry-mixing Ottawa sand and bentonite, at a skeleton relative density of $35\% \pm 5\%$. Two main variables are investigated: the percentage of bentonite (3% and 5% by dry mass of the sand), and the duration of the ageing period preceding shear (1 to 10 days). The presence of bentonite increases the shear strain needed to initiate the generation of excess pore pressures in resonant column tests; in cyclic tests it reduces the mean pore pressure generated per loading cycle and allows the specimen to sustain an increased loss of effective stress before liquefaction initiates, both effects contributing to an increased resistance to liquefaction. These effects are further enhanced with prolonged pre-shear ageing. Additionally, under static conditions, the behaviour of the sand is found to become increasingly stable as the ageing duration is extended. Given the role played by the ageing period, the effects observed cannot be simply ascribed to the increased bulk density of the specimens with bentonite. Instead, they are attributed to the pore fluid formed in presence of bentonite: a concentrated clay gel with solid-like properties. This pore fluid increases the sand's threshold shear strain, which is shown to have a strong correlation with the resistance to liquefaction.

KEYWORDS: laboratory tests; liquefaction; pore pressure; sands

INTRODUCTION

The issue of initiation and generation of excess pore pressure is critical in understanding and predicting the liquefaction phenomenon in sands and other granular materials under both static and cyclic loading.

For cyclic loading, two methods were used to study the rate and magnitude of pore pressure generation. The first method was stress-controlled cyclic tests, in which the generation of excess pore pressure was evaluated as a function of the number of loading cycles. The second method was strain-controlled cyclic tests with measurement of excess pore pressure with loading cycles for a given shear strain level.

Previous research (Lee & Albaisa, 1974; De Alba *et al.*, 1976; Seed *et al.*, 1976) showed a strong correlation between the normalised excess pore pressure ratio (the ratio between the measured excess pore pressure and the initial effective confining stress) and the number of loading cycles normalised by the number of cycles required to cause liquefaction. From undrained cyclic loading tests on Sacramento River and Monterey sands performed under stress control, Lee & Albaisa (1974) found a continuous increase in excess pore pressure as the cyclic loading progressed. They suggested that the excess pore pressure falls within a narrow band for a given sand, and is insensitive to the soil's initial density and consolidation

stress. Similar findings were reported by De Alba *et al.* (1976) for Monterey #0 sand.

Dobry *et al.* (1982) and Dobry (1985) examined pore pressure generation during strain-controlled, undrained cyclic loading as a function of the shear strain. They investigated the behaviour of saturated sands for a wide range of relative densities using different sands and various specimen preparation techniques. They too observed that the measured excess pore pressure fell within a narrow band, and found that it did not develop until a threshold shear strain was reached. Dobry (1985) referred to this strain as the threshold shear strain, and found it to be about 0.01%. Recent data (e.g. Hsu & Vucetic, 2004; Hazirbaba & Rathje, 2009) support this observation.

The presence of fines changes the response of sands during undrained loading, and numerous laboratory experimental investigations have explored this issue, focusing in particular on the effects of fines on cyclic resistance (e.g. Chang *et al.*, 1982; Troncoso & Verdugo, 1985; Law & Ling, 1992; Finn *et al.*, 1994; Koester, 1994; Vaid, 1994; Thevanayagam *et al.*, 2002; Carraro *et al.*, 2003; Polito & Martin, 2003). These studies paint a complex picture of behaviour in which the amount and the nature of the fines (plastic or non-plastic) play a critical role. The presence of fines also controls the undrained response under static loading (e.g. Georgiannou *et al.*, 1991; Yamamuro & Lade, 1998; Murthy *et al.*, 2007; Bobei *et al.*, 2009), and sands with fines have been shown to exhibit a 'reverse' (Yamamuro & Lade, 1998) pattern of pore pressure generation, with increased instability (i.e. a greater tendency to liquefy) at lower pre-shear effective stresses.

With regard to the effect of plastic fines, there is general consensus that their presence produces an increase in the resistance to liquefaction. This conclusion is supported by field observations (e.g. Wang, 1979; Seed *et al.*, 1983; Tokimatsu & Yoshimi, 1983; Ishihara, 1993, 1996) and laboratory data (e.g. Ishihara & Koseki, 1989; Yasuda *et al.*,

Manuscript received 12 November 2012; revised manuscript accepted 28 August 2013. Published online ahead of print 6 November 2013. Discussion on this paper closes on 1 July 2014, for further details see p. ii.

* Department of Civil, Architectural and Environmental Engineering, The University of Texas at Austin, TX, USA.

† School of Civil Engineering, Purdue University, West Lafayette, IN, USA.

‡ Department of Agronomy, Purdue University, West Lafayette, IN, USA.

1994). The latter includes work performed by the authors (El Mohtar *et al.*, 2008a, 2013; Rugg *et al.*, 2011) as part of an investigation on the use of bentonite suspensions to treat liquefiable soils. These showed that the presence of small percentages (3–5%) of bentonite, if properly hydrated, increased the cyclic resistance compared with clean sand at the same skeleton relative density, and that an extended duration of pre-shear ageing led to a further increase of the cycles required to liquefy the soil at a given cyclic stress ratio, CSR (Fig. 1).

In general, the impact of fines on pore pressure generation during cyclic loading has received less attention. Data by Polito (1999) on Yatesville sand showed that for kaolinite percentages up to 17% the curves of normalised excess pore pressure against normalised number of cycles fall within the band formed by the data for sand with no fines, and are within the range found in earlier studies as typical for clean sands. Additionally, these data indicate that an increasing plasticity of the fines leads to a faster rate of pore pressure generation during the first part of the test. As pointed out by Hazirbaba & Rathje (2009), few studies have investigated the effect of the fines on pore water pressure generation; in particular, very limited data are available on the effect of plastic fines on the threshold shear strain. The observed increase in threshold shear strain with increasing soil plasticity reported, for example, by Hsu & Vucetic (2006) for cohesive soils suggests that an increase in the threshold shear strain might be expected with increasing plasticity of the fines.

The work presented in this paper seeks to increase understanding of the mechanisms responsible for the development of excess pore pressure in sands with highly plastic fines. It examines the effects of the presence of bentonite – a highly plastic clay – on the initiation of excess pore pressure at small strains (from resonant column tests), on the pore pressure developed at large strains under monotonic loading (from static triaxial tests), and on the rate of pore pressure generation during cyclic loading all the way to liquefaction (from cyclic triaxial tests). It emphasises the effects of the microstructure, and in particular the role played by bentonite in the pore fluid on the overall macroscopic behaviour.

EXPERIMENTAL METHODS

Static triaxial, cyclic triaxial and resonant column tests were conducted on soil specimens prepared by mixing Ottawa sand with 3% and 5% bentonite by weight of dry sand. The sand used for the tests was Ottawa sand C 778, a

very uniform ($C_u = 1.7$), clean, fine-to-medium sand, with 2–5% non-plastic fines passing the no. 200 sieve, specific gravity (G_s) of 2.65, and maximum and minimum void ratios equal to 0.78 (e_{max}) and 0.48 (e_{min}) respectively. The bentonite used was a commercial Wyoming bentonite, manufactured by Volclay, with at least 85% passing the no. 200 sieve, specific gravity of 2.65 and liquid limit (LL) and plastic limit (PL) equal to 397% and 41% respectively. Bentonite consists primarily of smectite clay minerals, 2:1 minerals formed with an octahedral layer sandwiched between two tetrahedral layers.

The bentonite was introduced into the specimens by dry-mixing it with the sand at percentages of 3% or 5% with respect to the dry weight of the sand, before specimen preparation. The mixture was then air-pluviated into a standard, membrane-lined, split triaxial mould with a nominal diameter of 71 mm and height-to-diameter ratio of 2. Air pluviation consists of passing the dry-mixed soil through a funnel and tube into a mould.

After pluviation, a suction of 25 kPa was applied to allow for removal of the split mould, measurement of the specimen dimensions, and assembly of the triaxial cell. Then the suction was gradually replaced by a cell pressure of 25 kPa, maintaining a constant effective stress. The specimen was then flushed first with carbon dioxide and then with water from the bottom of the specimen under a low gradient (to minimise volume changes associated with flushing). Specimens with bentonite were allowed to hydrate for 72 h before back-pressure saturation; clean sand specimens were back-pressure saturated right after flushing with water. For all specimens, a minimum B -value of 0.95 was reached before the consolidation stages. Specimens were then consolidated to 100 kPa effective stress, left undisturbed for a period of time (ranging between 1 and 10 days), and then tested.

For tests with consolidation times exceeding 1 day, a layer of mineral oil was added on top of the water surrounding the specimen to reduce air migration through the water into the specimen. B -value measurements taken over a period of 10 days showed no change in the level of saturation, and the measured B -values remained above 0.95. All drainage lines were dry at the beginning of the test to avoid hydration of the bentonite near the top and bottom caps, which would interfere with carbon dioxide and water flushing. Additional details of specimen preparation and testing procedures can be found in El Mohtar (2008) and El Mohtar *et al.* (2013).

Clean sand and sand–bentonite specimens were prepared targeting the same end of consolidation (pre-shear) ‘skeleton void ratio’. This parameter is the void ratio calculated by neglecting the presence of the bentonite. The value of the targeted skeleton void ratio corresponds to a skeleton relative density of $35\% \pm 5\%$ (calculated using the minimum and maximum void ratios of the clean sand).

The initial weight and height measurements and the height and volume changes measured during the flushing, hydration and consolidation stages were used to track the specimen void ratio. At the conclusion of each test, the specimen was divided into three sections (top, centre and bottom), and the bentonite content and void ratio were measured for each section. The measured bentonite contents were within 0.5% (by dry mass of sand) of the target value. The void ratio was calculated from the measured water content at the three different locations (assuming saturation), and was found to be within $\pm 3\%$ of each specimen mean void ratio.

Multiple tests were performed at selected CSR values to ensure the repeatability of the results (CSR of 0.1 and 0.15 for sand, CSR of 0.1, 0.125, 0.1 and 0.2 for 3% bentonite specimens, and CSR of 0.2, 0.175 and 0.15 for 5% bentonite specimens).

In addition to the resonant column and triaxial tests,

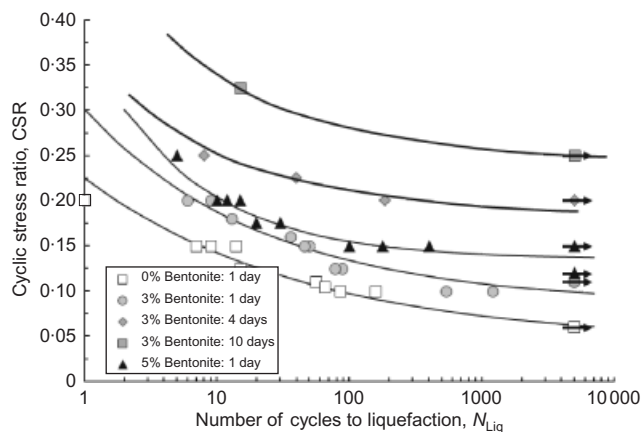


Fig. 1. Cyclic stress ratio against number of cycles with percentage of bentonite and ageing time (modified from El Mohtar *et al.*, 2013). All specimens prepared at skeleton relative density of $35\% \pm 5\%$. Arrows indicate tests that did not liquefy

rheological tests were performed on concentrated bentonite suspensions representative of the pore fluid formed in the sand–bentonite mixtures. These tests were conducted using the Anton Paar MCR 301 rheometer, a state-of-the-art apparatus through which the flow and viscoelastic properties of complex fluids can be measured. Specifically, the cone and plate geometry was employed to conduct amplitude sweep tests, which provide a measure of the stiffness of the bentonite suspension as a function of shear strain.

RESULTS

Pore pressure generation at small strains from resonant column tests

Specimens in the fixed-base, free-top resonant column test had dimensions similar to those for the triaxial tests, a nominal diameter of 71 mm and a height-to-diameter ratio of 2. Resonant column tests on clean Ottawa sand and sand with 3% and 5% bentonite were performed under undrained conditions to observe whether the shear strain threshold, at which specimens start to generate excess pore pressure, changes with the addition of bentonite. Fig. 2 shows plots of the excess pore pressure generated in sand specimens with 0% (clean sand), 3% and 5% bentonite at an effective confining stress of 100 kPa. The results show that excess pore pressure starts generating in clean sand specimens at lower shear strains relative to the sand–bentonite specimens. At any given strain exceeding the threshold shear strain for clean sand, the magnitude of the excess pore pressure is much larger in clean sand than in sand with bentonite.

Figure 2 also shows plots of normalised shear modulus as a function of shear strain. These plots show an increased linear threshold and a decreased degree of non-linearity for the sand–bentonite specimens compared with clean sand. The magnified loss in normalised shear modulus at higher shear strains is due primarily to the reduction in effective stresses caused by the generation of excess pore pressure. This can be observed from the results (Fig. 3) of resonant column tests conducted under drained conditions – that is, at a constant effective confining stress – on both clean sand and 3% bentonite specimens. Fig. 3 shows that under drained conditions the normalised shear modulus curves for the two specimens overlap, indicating that, at a constant effective stress, the presence of bentonite has no effect on the variation of the normalised shear modulus with shear strain. Also included in Fig. 3 are the curves for the same two specimens tested under undrained conditions. It is seen that the undrained data for the sand–bentonite specimen fall in the same band as the drained results. This is due to the limited excess pore pressures generated during testing for the range

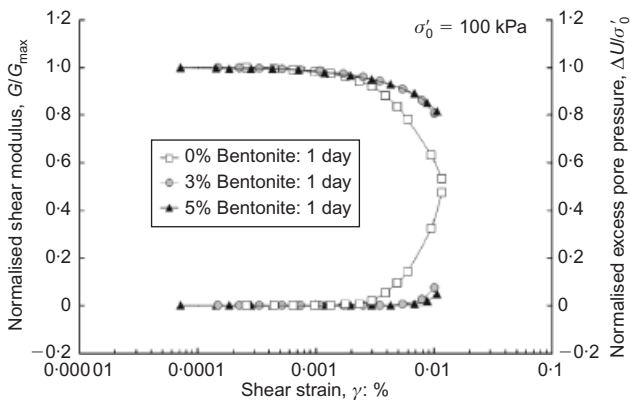


Fig. 2. Normalised shear modulus and excess pore pressure against shear strain from undrained resonant column tests

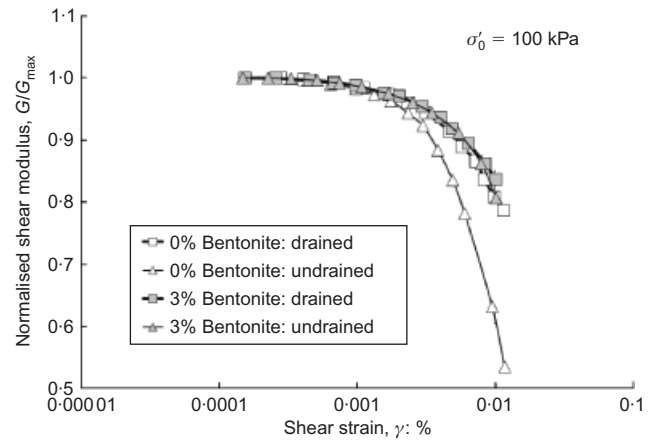


Fig. 3. Drained and undrained normalised shear modulus against shear strain for clean sand and 3% bentonite specimens from resonant column tests

of strains applied, which is in contrast to the clean sand response.

Undrained resonant column tests were also performed on specimens with 3% bentonite after 1, 4 and 10 days of ageing at an effective confining stress of 100 kPa. At the end of the ageing time, undrained resonant testing was done. Fig. 4 shows plots of the normalised shear modulus and the excess pore pressure, normalised by the pre-shear effective confining stress, against shear strain. The results for a test on clean sand are also included for comparison. While no significant change in the stiffness degradation curve is observed with increased ageing duration, the excess pore pressure data show a clear delay in pore pressure generation with increasing ageing. The values of the threshold shear strain summarised in Table 1 show an over fivefold increase in threshold strain from clean sand to 3% bentonite after 10 days of ageing.

Note that the value reported in Table 1 for clean sand is

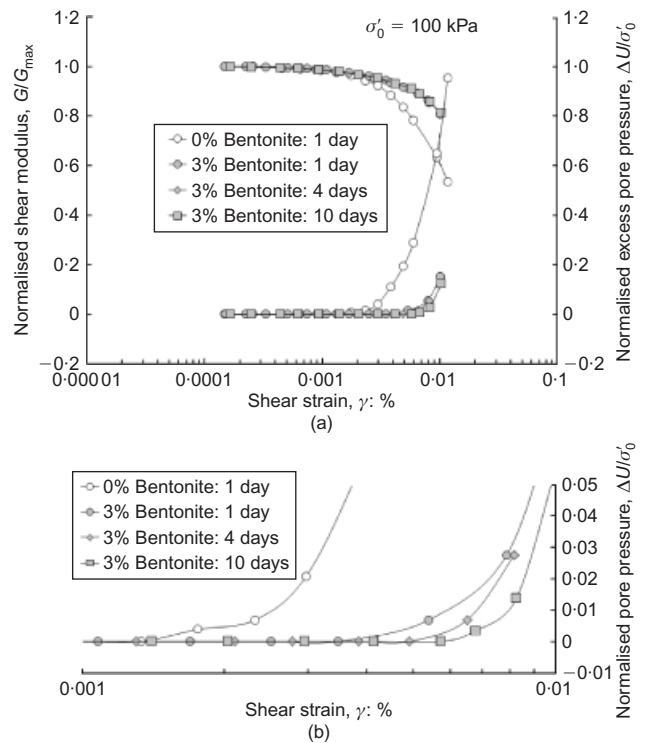


Fig. 4. (a) Normalised shear modulus and excess pore pressure and (b) normalised pore pressure against shear strain after 1, 4 and 10 days of ageing

Table 1. Variation of threshold shear strain (%) with bentonite content and ageing time

Clean sand	3% Bentonite: 1 day	5% Bentonite: 1 day	3% Bentonite: 4 days	3% Bentonite: 10 days
0.0013	0.0035	0.004	0.0049	0.006

approximately an order of magnitude smaller than the 0.01% threshold cyclic shear strain value cited, for example, by Dobry & Abdoun (2011). As discussed in detail by Chung *et al.* (1984), this is expected in tests on virgin specimens such as the ones presented in this paper, in which the excitation force is increased incrementally, with the drainage lines always remaining closed. Chung *et al.* reported a threshold cyclic shear strain amplitude of 0.0015% at which excess pore pressures started generating. At these small strain levels, the excess pore pressures are limited and cannot generate liquefaction, regardless of the number of loading cycles. Other factors that contribute to the difference between threshold shear strain in this study and the threshold shear strain reported in the literature (e.g. Dobry *et al.*, 1981) is that the resonant frequencies are at approximately 100 Hz (compared with 1 Hz), and that many cycles of loading, typically several thousands, occur for each data point on these plots. Nonetheless, the test results are reproducible and consistent, and are reliable measures of shear modulus and damping at very low to medium shear strains.

Pore pressure generation at large strains obtained from cyclic loading tests

The generation of excess pore pressure and its effect on the behaviour of sand–bentonite specimens at large strains were investigated by conducting stress-controlled undrained cyclic loading triaxial tests. As discussed earlier, evaluation of the pore pressure response during cyclic loading is traditionally based on plotting data in terms of excess pore pressure normalised by the initial confining effective stress against the number of cycles normalised by the number of cycles necessary to generate liquefaction (for all tests in this study, liquefaction was defined as the condition correspond-

ing to the excess pore pressure reaching 100% of the initial lateral effective stress). Fig. 5 compares the response of clean sand and sand with 3% and 5% bentonite after 1 day of consolidation. For reference, the figure also includes an envelope based on data from the literature for different clean sands (Lee & Albaisa, 1974; De Alba *et al.*, 1976). The data for the clean sand fall in the range for other clean sands reported in the literature, while the 3% and 5% bentonite bands are shifted upwards, owing to a higher rate of excess pore pressure generation in the earlier cycles. However, the rate of pore pressure generation slows down after that initial phase, resulting in the increased cyclic resistance observed in Fig. 1.

Additional insight into the role played by the bentonite fines can be obtained by looking more closely at the different stages of excess pore pressure generation, which are identified in Fig. 6(a). The plot of excess pore pressure against number of cycles shown in this figure pertains to a 3% bentonite specimen tested with a CSR of 0.125 after 1 day of ageing. The excess pore pressure generated during cyclic loading can be separated into two components: (a) the component associated with the loading cycle (U_{cyclic}) – that is, the temporary excess pore pressure that is dissipated at the end of each loading cycle; and (b) the mean excess pore pressure (U_m), which is non-recoverable, and is continued to the next cycle.

Four distinct regions can be identified in the excess pore pressure curve presented in Fig. 6(a), as follows.

- (a) An initial relatively short region in which the development of mean excess pore pressure accelerates with every cycle.
- (b) An extended plateau characterised by an almost constant rate of mean excess pore pressure generation with each cycle; this region ends at N_{Acc} number of cycles.

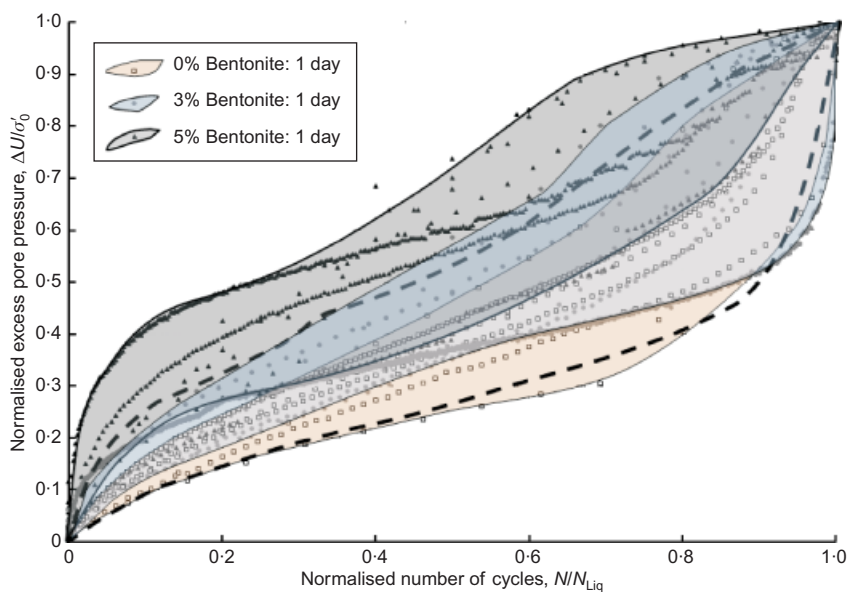


Fig. 5. Normalised mean excess pore pressure against normalised number of cycles to liquefaction for clean sand and sand–bentonite specimens. Dashed lines represent the range for clean sand from the literature

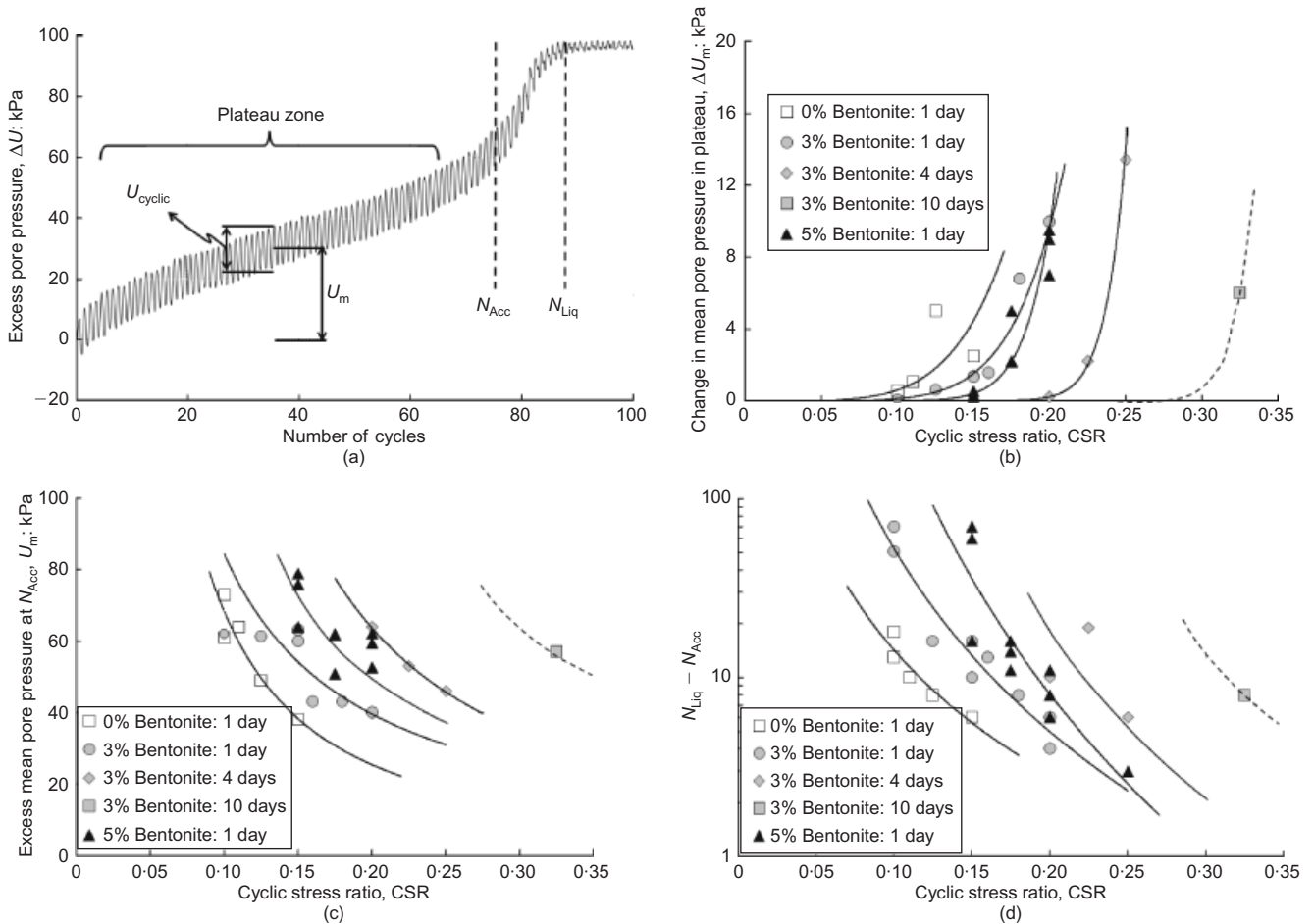


Fig. 6. (a) Typical pattern of excess pore pressure generation in a cyclic test. Effect of pore fluid on excess mean pore pressure generation: (b) in plateau region; (c) at N_{Acc} ; (d) on number of cycles from N_{Acc} to N_{Liq} (solid lines, power functions to fit the data; dashed lines, expected trends due to limited data points)

- (c) A region extending between cycles N_{Acc} and N_{Liq} , in which the pore pressure generation is accelerated until the soil liquefies (liquefaction is defined in correspondence to zero effective confining stress).
- (d) A post-liquefaction phase during which there is no change in the mean excess pore pressure; this is the region beyond N_{Liq} number of cycles.

All clean sand, 3% and 5% bentonite specimens that reached liquefaction displayed a similar pore pressure generation curve except for specimens that liquefied in less than 10 cycles (insufficient cycles to identify the four distinct regions).

As shown in Fig. 5, an initial higher rate of pore pressure generation is observed in the sand–bentonite specimens. This behaviour can be attributed to the presence of bentonite particles trapped at the sand contacts, which, as reported by El Mohtar *et al.* (2008b), also causes the initial stiffness of the specimen measured in resonant column tests to decrease slightly; this results in higher deformations and excess pore pressure generation. Beyond this stage, which is limited to less than 15% of the cycles required to liquefy the specimen, the presence of bentonite reduces the excess pore pressure generation under the applied cyclic loads. This is shown in Fig. 6(b), which presents the average mean excess pore pressure generated per loading cycle in the plateau region against the CSR. The figure, which includes results from specimens prepared with 0%, 3% and 5% bentonite tested after 1 day of consolidation, as well as those from 3% bentonite specimens tested after 4 and 10 days of consolidation, shows that for all the specimens there is an exponential

increase in the average mean excess pore pressure with increasing CSR. More importantly, it shows that at any CSR there is a significant decrease of the mean excess pore pressure with increasing bentonite content and/or ageing of the bentonite. In addition to reducing excess pore pressure generation in the plateau region, the presence of bentonite and prolonged ageing essentially ‘extend’ this region. This is illustrated in Fig. 6(c), which shows the magnitude of the mean excess pore pressure, ΔU_m , developed at cycle N_{Acc} for different bentonite contents and ageing times. N_{Acc} , which is the number of cycles at which the generation of excess pore pressure generation starts accelerating, was identified by plotting the change in mean excess pore pressure (U_m) against loading cycle, as shown in Fig. 7 for two tests: one on clean sand (Fig. 7(a)), which liquefied after 15 cycles, and the other (Fig. 7(b)) on a specimen with 3% bentonite, in which liquefaction was reached after 88 cycles, both tested at a CSR of 0.125.

Figure 6(c) shows that, for a given CSR, N_{Acc} occurs at higher mean excess pore pressure, ΔU_m , with increasing bentonite content and ageing time. This indicates that increasing bentonite content and/or ageing results in specimens that are able to sustain a greater loss in effective confining stress before reaching N_{Acc} , that is, before the excess pore pressure generation accelerates. Differences in excess pore pressure generation in the presence of bentonite are observed even after the specimens have reached cycle N_{Acc} . Consistent with the reduced rate of excess pore pressure generation in this region shown in Fig. 5, it is found that, in the case of clean sand, fewer cycles are needed to go from cycle N_{Acc} to N_{Liq} than in the case of

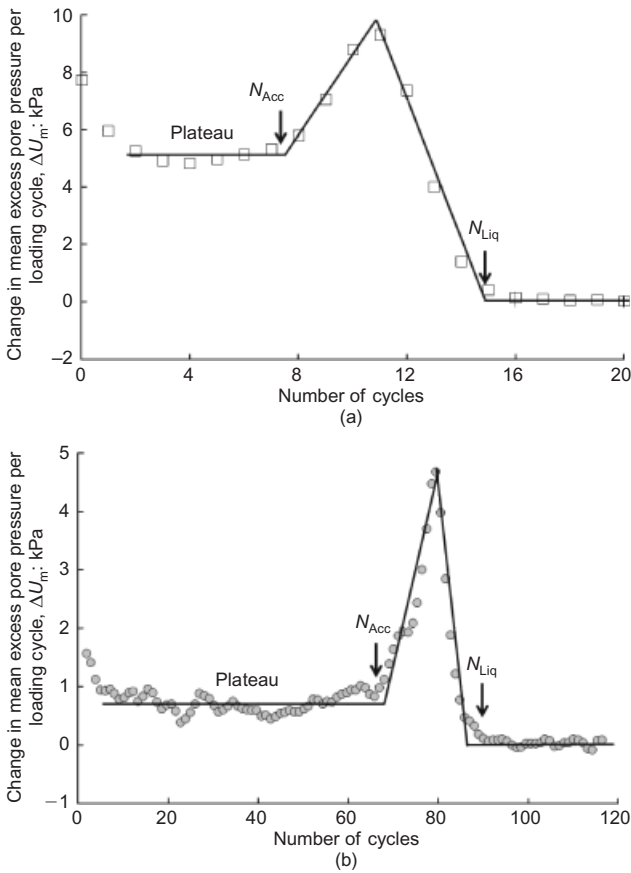


Fig. 7. Change in mean excess pore pressure generation per loading cycle for (a) clean sand and (b) 3% sand-bentonite specimen, both loaded at CSR of 0.125

specimens with bentonite. This is shown in Fig. 6(d), which plots the number of loading cycles needed to cause liquefaction beyond N_{Acc} (i.e. $N_{Liq} - N_{Acc}$) with increasing bentonite content and ageing duration. The combination of the effects outlined in Fig. 6 produces the increased resistance to liquefaction depicted in Fig. 1.

Pore pressure generation at large strains from static loading tests

A series of undrained isotropically consolidated static triaxial tests was performed to characterise the mechanical properties of the sand-bentonite mixtures, and to determine the effects of bentonite and ageing on the excess pore pressure generation under static loading. Tests were run on specimens with 0%, 3% and 5% bentonite content at confining stresses of 50 kPa, 100 kPa and 150 kPa. Additional 3% bentonite specimens were allowed different ageing times, ranging from 1 to 10 days, under a constant 100 kPa effective confining stress. Fig. 8 shows plots of the excess pore pressure generated during the undrained static shear, and Fig. 9 shows the corresponding stress paths. Fig. 8 shows a more contractive tendency for the 3% and 5% bentonite specimens tested after 1 day of consolidation than clean sand before the phase transformation and the start of dilation; additionally, the 3% specimens consistently show a marginally higher excess pore pressure than the 5% bentonite specimen at any strain level. Similar trends are observed at 50 kPa and 150 kPa. The opposite effect is observed when the specimens are allowed to age for extended periods. As shown in the figure, the excess pore pressure decreases significantly with increased ageing: for example, Fig. 8 shows that, for the same 3% bentonite content after 10 days

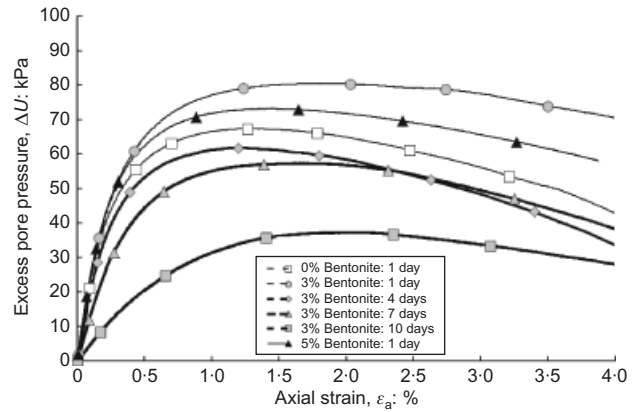


Fig. 8. Excess pore pressure generation for clean sand and sand-bentonite specimens from undrained triaxial compression tests

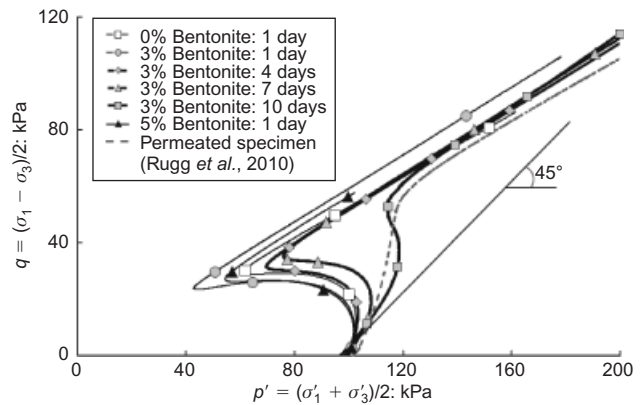


Fig. 9. Stress paths for clean sand and sand-bentonite specimens from undrained triaxial compression tests

of consolidation, the excess pore pressure generated is less than half of that generated after 1 day of ageing.

It is suggested that the increased generation of excess pore pressure in the specimens with 3% and 5% bentonite tested after 1 day of consolidation is due to the bentonite trapped between the sand grains during specimen formation. With continued shear the grain contacts can engage, eventually producing the shift from contractive to dilatant tendency. This is similar to what has been observed, for example, by Yamamuro & Lade (1998) in undrained tests on sand with silty fines. This hypothesis is supported by the results of undrained tests conducted by Rugg *et al.* (2011) on specimens of Ottawa sand permeated with bentonite suspensions, in which an amount of bentonite corresponding to 3% by dry mass of the sand was delivered in the pore space in the form of a suspension after formation of the clean sand specimen. Given the delivery of the bentonite through permeation, the sand skeleton structure of this specimen was not altered, and the increased contractive tendency observed above for the dry-mixed specimens with 1 day of ageing was not observed.

Figure 9 also shows that with an increase in ageing time the specimens become less contractive, and that the dilation tendency starts at a higher mean effective stress. After 10 days of ageing the response of the sand-bentonite specimen resembles that observed for the permeated specimen tested by Rugg *et al.* (2011). This is an indication that at this time the response is fully controlled by the pore fluid.

The change in behaviour with ageing at the same bentonite content and same effective confining stress also implies

that the properties of the clay between sand grains and the pore fluid control the contractive/dilative tendency rather than the absolute change in bulk density due to the presence of the fines. Fig. 9 also indicates that clay percentage and ageing time affect the peak friction angle. This influence requires further investigation.

MICROSTRUCTURE AND PORE PRESSURE GENERATION

The results presented above show that the addition of small percentages (3–5%) of bentonite produces significant changes in the response of sand at both small and large strains. Most importantly, from a practical perspective, the addition of bentonite leads to an increase in cyclic resistance at any given CSR. Moreover, for a given bentonite percentage, the resistance to liquefaction increases with time (Fig. 1). It is proposed that the observed changes in behaviour are due to the swelling of the bentonite inside the sand pore space and the formation of a thixotropic pore fluid of concentrated bentonite suspension.

Oscillatory rheological tests conducted on concentrated bentonite suspensions provide the means to investigate the mechanical properties of the pore fluid that is formed under these conditions. For the targeted skeleton relative density of 35%, the concentration of bentonite in the pore fluid is calculated at approximately 10% and 16.7% (by mass of the water) for bentonite contents equal to 3% and 5% by mass of the sand respectively. These calculations assume that all the bentonite hydrates and swells inside the sand pore space. Previous work (El Mohtar *et al.*, 2008a, 2013) suggests that this may not be the case because of the specimen preparation procedure followed, which allows part of the bentonite to remain attached to the surface of the sand grains. Regardless, similar observations would apply for slightly less concentrated suspensions.

Figure 10 shows curves of the storage (elastic) and loss (viscous) moduli determined from amplitude sweep tests performed on 10% and 16.7% bentonite suspensions (two independent tests for each concentration). These tests involved application of a sinusoidal shear strain of increasing amplitude at a frequency of 1 Hz, and measurement of the resulting shear stress, which can be expressed as the sum of two components: one in phase with the applied shear strain, from which the storage modulus (G') is derived; and one 90° out of phase, from which the loss modulus (G'') is calculated. The figure shows an essentially linear elastic response ($G' = \text{constant}$ and $\gg G''$) for shear strains up to 1%, solid-like behaviour (i.e. $G' > G''$) up to shear strains exceeding 10%,

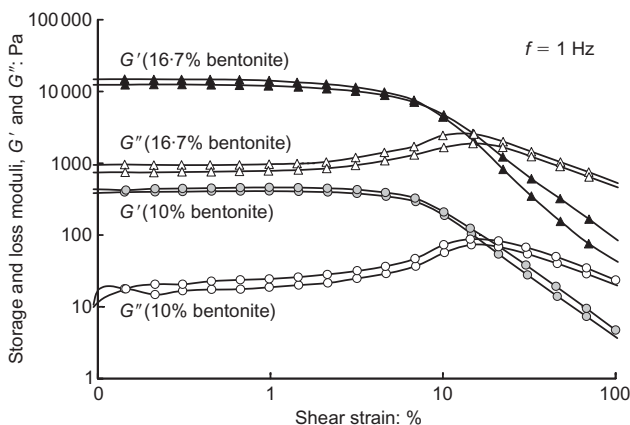


Fig. 10. Storage and loss moduli for 10% and 16.7% bentonite suspensions from rheological tests

and a significant increase in storage modulus with increasing bentonite content. The data shown in Fig. 10 pertain to suspensions tested 1 day after being mixed. With increased ageing time both moduli increase significantly (Clarke, 2008).

The behaviour shown in Fig. 10 is typical of materials termed 'gels' (e.g. Abend & Lagaly, 2000) or also 'soft jammed systems' (Coussot, 2005), in which each of the colloidal-size particles (bentonite in this case) interacts with a number of the other elements that surround it. It is the 'jammed' nature of this pore fluid that limits the movement of the sand particles.

The plots of storage modulus (G') against shear strain for 10% and 16% bentonite suspensions are shown in Fig. 11, together with a plot of the shear modulus (G), against shear strain for a clean sand specimen tested at a confining stress of 100 kPa. The shear modulus curve for the clean sand was obtained by combining the results from an undrained resonant column test ($\gamma < 10^{-2}\%$) and an undrained cyclic triaxial test ($\gamma > 10^{-2}\%$). Young's modulus and axial strains were converted to shear modulus and shear strains respectively, assuming isotropic linear elastic behaviour with a Poisson's ratio of 0.5, as described by Georgiannou *et al.* (1991). This representation enables a comparison of behaviour with increasing shear strain between the sand skeleton and the bentonite-rich pore fluid in the sand–bentonite mixtures. Fig. 11 shows that the mixtures are composed of a stiff sand skeleton with a small elastic threshold ($< 0.005\%$) and a much 'softer' pore fluid with a high linear elastic threshold ($> 1\%$).

Figure 11 suggests that during cyclic loading, once the shear strain exceeds the linear threshold of the sand, the pore fluid provides an elastic restraint to particle movement, thus reducing plastic deformations in the specimen. This hypothesis is consistent with the increase in the threshold shear strain (corresponding to the onset of excess pore pressure generation during undrained loading), with increasing bentonite content observed in resonant column tests (Table 1). The hypothesis is also supported by the behaviour observed with increased ageing, as the shear stiffness of the pore fluid increases, providing additional resistance to particle movement, and resulting in an increase in the threshold shear strain as well.

RELATING SMALL- AND LARGE-STRAIN RESPONSE

The results for the resonant column tests performed under undrained conditions reported above show that the presence of bentonite leads to an increase in the threshold shear strain required to initiate excess pore pressures. Extended ageing

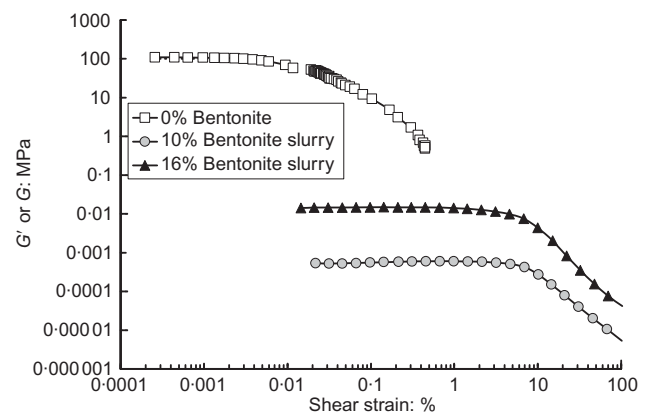


Fig. 11. Shear stiffness against shear strain for sand skeleton (from resonant column and cyclic triaxial tests) and for bentonite pore fluid (from rheological tests)

further causes this strain to increase, by as much as a factor of 5 for the testing conditions examined in this paper.

The increase in the threshold shear strain is thought to be one of the mechanisms responsible for the increase in liquefaction resistance of the sand–bentonite specimens. This is illustrated in Figs 12 and 13, which show how both the double-amplitude shear strain measured at cycle N_{Acc} and the number of cycles to liquefaction measured in cyclic triaxial tests exhibit a strong correlation with the threshold shear strain value measured in resonant column tests.

Figure 12 presents the values of CRR_{10} , CRR_{20} and CSR_{min} against threshold shear strain for clean sand, 3% sand–bentonite and 5% sand–bentonite specimens after 1 day of consolidation and 3% sand–bentonite specimens after 4 and 10 days of consolidation. CRR_{10} and CRR_{20} are the CSR values at which the soil reaches liquefaction in 10 and 20 cycles respectively, and CSR_{min} is the minimum CSR value needed to liquefy the soil. The results show a clear relationship between the cyclic resistance to liquefaction and the threshold shear strain: the higher the threshold shear strain, the greater the increase in cyclic resistance. This relationship between threshold shear strain and cyclic resistance is consistent with results published by Dobry *et al.* (1981), which show an increase in cyclic resistance of over-consolidated sands accompanied by an increase in the threshold shear strain.

Figure 13 shows the double-amplitude shear strain at cycle N_{Acc} (which for a given material is independent of CSR) against the threshold shear strain. While the two strains are

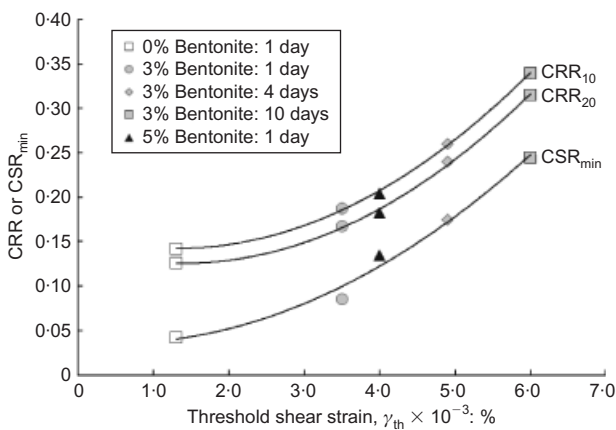


Fig. 12. Change in cyclic resistance and CSR_{min} as a function of threshold shear strain

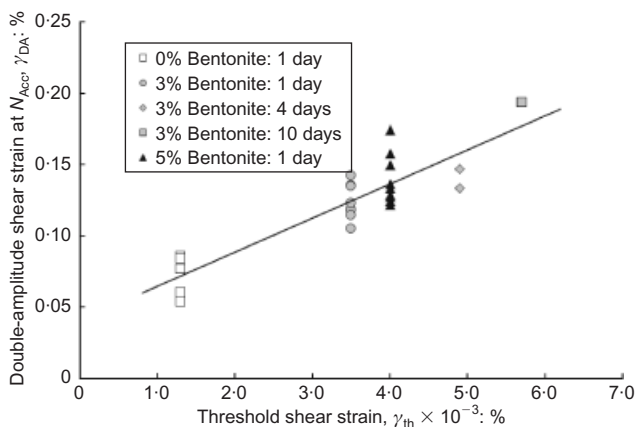


Fig. 13. Double-amplitude strain at N_{Acc} against threshold shear strain for 0%, 3% and 5% sand–bentonite specimens (solid line is linear best-fit line)

more than an order of magnitude apart, the figure shows that there is a strong correlation between threshold shear strain and the double-amplitude strain at cycle N_{Acc} . The higher double-amplitude strain at cycle N_{Acc} is consistent with the results presented in Fig. 6(c): given that specimens with bentonite can sustain higher shear strains before reaching cycle N_{Acc} , the generated excess pore pressures at this cycle are higher.

CONCLUSIONS

The paper presents the results of resonant column, static triaxial and cyclic triaxial tests on clean Ottawa sand and sand with 3–5% bentonite (by dry weight of the sand). All specimens were prepared at the same skeleton relative density ($35\% \pm 5\%$) by dry-mixing the sand and bentonite prior to specimen formation, and, for the specimens with bentonite, varying the duration of the post-consolidation ageing phase between 1 and 10 days.

The results show that the presence of the highly plastic fines significantly affects the generation of excess pore pressure at both small and large strains under static and cyclic loading.

Initially, the presence of bentonite results in a more contractive soil tendency (as compared with clean sand) under static loading. However, over time, the behaviour became less contractive, and excess pore pressures are reduced. This trend of reduced contractive tendency is a result of the change in the properties of the pore fluid rather than the bulk void ratio, since the latter does not change with time.

During undrained cyclic loading, both clean sand specimens and specimens with bentonite exhibit a similar pattern of excess pore pressure generation, consistent with data reported in the literature. However, the presence of bentonite and the duration of ageing affect the magnitude of the pore pressure during all stages of the test. Specifically, an increased bentonite content or extended ageing time reduces the rate of pore pressure generation during cyclic loading, allowing the soil to sustain a more significant effective stress loss prior to the acceleration of excess pore pressure generation, and increase the number of cycles that the soil can sustain thereafter, prior to liquefying. Combined, these three effects contribute to a dramatic increase in the liquefaction resistance of the sand.

These results are consistent with field observations of the increased liquefaction resistance of deposits with plastic fines, and support the use of a recently proposed liquefaction mitigation technique (El Mohtar *et al.*, 2013), which is based on introducing small percentages of bentonite into the soil’s pore space.

The significant role played by ageing duration indicates that, for the high-plasticity fines examined in this research, the observed changes in material response are not influenced by changes in the bulk density of the soil. Instead, they appear to be controlled by the properties of the pore fluid formed in the presence of bentonite: a concentrated clay gel, which exhibits elastic behaviour up to shear strains exceeding 1%. The formation of this pore fluid is responsible for the increase in the critical strain at which excess pore pressure is generated, as observed in the resonant column tests. An extended duration of the ageing time further increases the value of this threshold shear strain, which is found to have a strong correlation with the soil’s resistance to liquefaction.

The impact of the ageing duration demonstrated in the paper indicates that previous studies that have not specifically addressed the role of ageing may not adequately represent field conditions. It also suggests that inconsisten-

cies in laboratory observations on the effects of plastic fines reported in the literature (e.g. Chang *et al.*, 1982; Troncoso & Verdugo, 1985) could be a result of different durations of the post-consolidation ageing phase.

ACKNOWLEDGEMENTS

This research was supported by the National Science Foundation, Geomechanics and Geotechnical Systems Programme, under grant CMS-0408739. This support is gratefully acknowledged. Special thanks go to Ms J. P. Clarke for her work on the rheology of bentonite suspensions.

NOTATION

C_u	coefficient of uniformity
e_{\max}	maximum void ratio
e_{\min}	minimum void ratio
G	shear modulus
G'	storage/elastic modulus
G''	loss/viscous modulus
G_{\max}	maximum shear modulus (at very small shear strains)
G_s	specific gravity
G/G_{\max}	normalised shear modulus
N	number of loading cycles
N_{Acc}	number of loading cycles beyond which rate of excess pore pressure generation accelerates
N_{Liq}	number of cycles to reach liquefaction
N/N_{Liq}	number of loading cycles normalised by number of cycles to reach liquefaction
p'	average principal effective stress ($= (\sigma'_1 - \sigma'_3)/2$)
q	shear stress ($= (\sigma_1 - \sigma_3)/2$)
U_{cyclic}	temporary excess pore pressure dissipated at end of each loading cycle
U_m	mean excess pore pressure
ΔU	excess pore pressure
$\Delta U/\sigma'_0$	normalised excess pore pressure
γ	shear strain
γ_{th}	threshold shear strain
γ_{DA}	double-amplitude shear strain
ε_a	axial strain
σ'_0	effective confining stress at end of consolidation
σ_1	major principal total stress
σ'_1	major principal effective stress
σ_3	minor principal total stress
σ'_3	minor principal effective stress

REFERENCES

- Abend, S. & Lagaly, G. (2000). Sol-gel transitions of sodium montmorillonite dispersions. *Appl. Clay Sci.* **16**, No. 3–4, 201–227.
- Bobei, D. C., Lo, S. R., Wanatowski, D., Gnanendran, C. T. & Rahman, M. M. (2009). Modified state parameter for characterizing static liquefaction of sand and fines. *Can. Geotech. J.* **46**, No. 3, 281–295.
- Carraro, J. A. H., Bandini, P. & Salgado, R. (2003). Liquefaction resistance of clean and nonplastic silty sands based on cone penetration resistance. *J. Geotech. Geoenviron. Engng* **129**, No. 11, 965–976.
- Chang, N. Y., Yeh, S. T. & Kaufman, L. P. (1982). Liquefaction potential of clean and silty sands. *Proceedings of the 3rd international earthquake microzonation conference*, Seattle, WA, USA, pp. 1017–1032.
- Chung, R. M., Yokel, F. & Wechsler, H. (1984). Pore pressure buildup in resonant column tests. *J. Geotech. Engng, ASCE* **110**, No. 2, 247–261.
- Clarke, J. (2008). *Investigation of time-dependent rheological behavior of sodium pyrophosphate–bentonite suspension*. Masters thesis, Purdue University, West Lafayette, IN, USA.
- Coussot, P. (2005). *Rheometry of pastes, suspensions and granular materials: Applications in industry and environment*. Wiley, New York, NY, USA.
- De Alba, P., Seed, H. B. & Chan, C. K. (1976). Sand liquefaction in large-scale simple shear tests. *J. Soil Mech. Found. Div., ASCE* **102**, No. GT9, 909–927.
- Dobry, R. (1985). *Liquefaction of soils during earthquakes*, National Research Council (NRC), Committee on Earthquake Engineering, Report No. CETS-EE-001. Washington, DC, USA: National Academy Press.
- Dobry, R. & Abdoun, T. (2011). An investigation into why liquefaction charts work: a necessary step toward integrating the states of art and practice. *Proceedings of the 5th international conference on earthquake geotechnical engineering*, Santiago, Chile, pp. 13–44.
- Dobry, R., Yokel, F. Y. & Ladd, R. S. (1981). Liquefaction potential of overconsolidated sands in areas with moderate seismicity. In *Earthquakes and earthquake engineering: The eastern United States* (ed. J. E. Beavers), vol. 2, pp. 642–664. Ann Arbor, MI, USA: Ann Arbor Science Publishers.
- Dobry, R., Ladd, R., Yokel, F., Chung, R. & Powell, D. (1982). *Prediction of pore water pressure buildup and liquefaction of sands during earthquakes by the cyclic strain method*, National Bureau of Standards, Building Science Series 138. Washington, DC, USA: US Department of Commerce.
- El Mohtar, C. (2008). *Pore fluid engineering: An auto-adaptive design for liquefaction mitigation*. PhD dissertation, Purdue University, West Lafayette, IN, USA.
- El Mohtar, C., Bobet, A., Santagata, M., Drnevich, V. & Johnston, C. (2008a). Cyclic response of sand with thixotropic pore fluid. In *Geotechnical earthquake engineering and soil dynamics IV* (eds D. Zeng, M. T. Manzari and D. R. Hiltunen), Geotechnical Special Publication 181 (CD-ROM). Reston, VA, USA: ASCE.
- El Mohtar, C., Santagata, M., Bobet, A., Drnevich, V. & Johnston, C. (2008b). Effect of plastic fines on the small strain stiffness of sand. *Proceedings of the 4th international symposium on deformation characteristics of geomaterials*, Atlanta, GA, USA, pp. 245–251.
- El Mohtar, C., Bobet, A., Santagata, M., Drnevich, V. & Johnston, C. (2013). Liquefaction mitigation using bentonite suspensions. *ASCE J. Geotech. Geoenviron. Engng* **139**, No. 8, 1369–1380.
- Finn, W. L., Ledbetter, R. H. & Wu, G. (1994). Liquefaction in silty soils: design and analysis. In *Ground failures under seismic conditions* (eds S. Prakash and P. Dakoulas), Geotechnical Special Publication 44, pp. 51–76. New York, NY, USA: ASCE.
- Georgiannou, V. N., Hight, D. W. & Burland, J. B. (1991). Behaviour of clayey sands under undrained cyclic triaxial loading. *Géotechnique* **41**, No. 3, 383–393, <http://dx.doi.org/10.1680/geot.1991.41.3.383>.
- Hazirbaba, K. & Rathje, E. M. (2009). Pore pressure generation of silty sands due to induced cyclic shear strains. *J. Geotech. Geoenviron. Engng, ASCE* **135**, No. 12, 1892–1905.
- Hsu, C.-C. & Vucetic, M. (2004). Volumetric threshold shear strain for cyclic settlement. *J. Geotech. Geoenviron. Engng, ASCE* **130**, No. 1, 58–70.
- Hsu, C.-C. & Vucetic, M. (2006). Threshold shear strain for cyclic pore-water pressure in cohesive soils. *J. Geotech. Geoenviron. Engng, ASCE* **132**, No. 10, 1325–1335.
- Ishihara, K. (1993). Liquefaction and flow failure during earthquakes. *Géotechnique* **43**, No. 3, 351–415, <http://dx.doi.org/10.1680/geot.1993.43.3.351>.
- Ishihara, K. (1996). *Soil behaviour in earthquake geotechnics*, 1st edn. Oxford, UK: Clarendon Press.
- Ishihara, K. & Koseki, J. (1989). Discussion of cyclic shear strength of fines-containing sands. *Proceedings of the 12th international conference on soil mechanics and foundation engineering*, Rio de Janeiro, Brazil, pp. 101–106.
- Koester, J. P. (1994). The influence of fine type and content on cyclic strength. In *Ground failures under seismic conditions* (eds S. Prakash and P. Dakoulas), Geotechnical Special Publication 44, pp. 17–33. New York, NY, USA: ASCE.
- Law, K. T. & Ling, Y. H. (1992). Liquefaction of granular soils with non-cohesive and cohesive fines. *Proceedings of the 10th world conference on earthquake engineering*, Rotterdam, the Netherlands, pp. 1491–1496.
- Lee, K. L. & Albaisa, A. (1974). Earthquake induced settlements in saturated sands. *J. Geotech. Engng Div., ASCE* **100**, No. 4, 387–406.
- Murthy, T. G., Loukidis, D., Carraro, J. A. H., Prezzi, M. & Salgado, R. (2007). Undrained monotonic response of clean and silty sands. *Géotechnique* **57**, No. 3, 273–288, <http://dx.doi.org/10.1680/geot.2007.57.3.273>.

- Polito, C. P. (1999). *The effects of non-plastic and plastic fines on the liquefaction of sandy soils*. PhD thesis, Virginia Polytechnic Institute and State University, Blacksburg, VA, USA.
- Polito, C. P. & Martin, J. R. (2003). A reconciliation of the effects of non-plastic fines on the liquefaction resistance of sands reported in the literature. *Earthquake Spectra* **19**, No. 3, 635–651.
- Rugg, D. A., Yoon, J., Hwang, H. & El Mohtar, C. S. (2011). Undrained shearing properties of sand permeated with a bentonite suspension for static liquefaction mitigation. In *Geofrontiers 2011: Advances in geotechnical engineering* (eds J. Han and D. A. Alzamora), Geotechnical Special Publication 211, pp. 677–686 (CD-ROM). Reston, VA, USA: ASCE.
- Seed, H. B., Martin, P. P. & Lysmer, J. (1976). Pore-water pressure changes during soil liquefaction. *J. Geotech. Engng Div., ASCE* **102**, No. GT4, 323–346.
- Seed, H. B., Idriss, I. M. & Arango, I. (1983). Evaluation of liquefaction potential using field performance data. *J. Geotech. Engng, ASCE* **109**, No. 3, 458–482.
- Thevanayagam, S., Shenthan, T., Mohan, S. & Liang, J. (2002). Undrained fragility of clean sands, silty sands, and sandy silts. *J. Geotech. Geoenviron. Engng* **128**, No. 10, 849–859.
- Tokimatsu, K. & Yoshimi, Y. (1983). Empirical correlation of soil liquefaction based on SPT N-value and fines content. *Soils Found.* **23**, No. 4, 56–74.
- Troncoso, J. H. & Verdugo, R. (1985). Silt content and dynamic behavior of tailing sands. *Proceedings of the 11th international conference on soil mechanics and foundation engineering*, San Francisco, CA, USA, pp. 1311–1314.
- Vaid, V. P. (1994). Liquefaction of silty soils. In *Ground failures under seismic conditions* (eds S. Prakash and P. Dakoulas), Geotechnical Special Publication 44, pp. 1–16. New York, NY, USA: ASCE.
- Yamamoto, J. & Lade, P. (1998). Steady-state concepts and static liquefaction of silty sands. *J. Geotech. Geoenviron. Engng, ASCE* **124**, No. 9, 868–877.
- Yasuda, S., Wakamatsu, K. & Nagase, H. (1994). Liquefaction of artificially filled silty sands. In *Ground failures under seismic conditions* (eds S. Prakash and P. Dakoulas), Geotechnical Special Publication 44, pp. 91–104. New York, NY, USA: ASCE.
- Wang, W. (1979). *Some findings in soil liquefaction*. Beijing, China: Water Conservancy and Hydroelectric Power Scientific Research Institute.